Inorganica Chimica Acta 415 (2014) 69–74

Contents lists available at ScienceDirect

Inorganica Chimica Acta

journal homepage: www.elsevier.com/locate/ica

# 1,2-Bis(diphenylphosphino)ethane nickel(II)dithiocarbamate as potential precursor for nickel sulfide: Effect of counter anion on phase and morphology

Ratna Chauhan [a], Manoj Trivedi [b], Jyoti Singh [b], Kieran C. Molloy [c], Gabriele Kociok-Köhn [c], Uttamrao P. Mulik [a], Dinesh P. Amalnerkar [a], Abhinav Kumar [d,*]

[a] Centre for Materials for Electronics Technologies, Pune, India
[b] Department of Chemistry, University of Delhi, Delhi, India
[c] Department of Chemistry, University of Bath, Claverton Down, Bath BA2 7AY, UK
[d] Department of Chemistry, Faculty of Science, University of Lucknow, Lucknow 226 007, India

ARTICLE INFO

*Article history:*
Received 11 December 2013
Received in revised form 11 February 2014
Accepted 16 February 2014
Available online 12 March 2014

*Keywords:*
dppe
Ni(II)
X-ray crystallography
TGA–DTA
NiS

ABSTRACT

One heteroleptic Ni(II)dppe dithiocarbamate complex cation $[Ni\{S_2CN(CH_2)_4CHOH)\}(dppe)]^+$ with three different counter anions *viz.* $PF_6^-$ (**1**), $BPh_4^-$ (**2**) and $BF_4^-$ (**3**) have been synthesized and characterized by microanalysis, IR, UV–Vis, $^1H$, $^{13}C$ and $^{31}P$ NMR spectroscopy and X-ray crystallography. The crystal structure of **2** displayed distorted square planar geometry around Ni(II) center bonded through sulfur atoms of the dithiocarbamate ligand and two phosphorus atoms of the dppe. TGA results indicated that all the three compounds display loss of solvents at the outset and decompose to Ni–S phase systems. The nickel sulfides obtained from decomposition of **1–3** have been characterized by pXRD and SEM. The effect of the bulkiness of the counter anions on the phase and morphology of decomposed product have been observed using pXRD and SEM analysis. The UV–Vis and photoluminescent spectroscopy of the three decomposed product have been performed.



## 1. Introduction

Nickel sulfide is known to have various stoichiometries: $Ni_3S_2$, $Ni_{3+x}S_2$, $Ni_4S_{3+x}$, $Ni_6S_5$, $Ni_7S_6$, $Ni_9S_8$, $Ni_3S_4$, $NiS_2$ and NiS [1–5]. These differing stoichiometries make nickel sulfide attractive and potentially important material in a diverse number of technical applications such as electrodes, battery materials, hydrogenation catalysts, and transformation toughening for complex ceramics [6–9]. They can also be the potential competitor for silicon in thin film solar cells [10]. Various methods have been used to synthesize nickel sulfide nanostructures. A solvothermal method was used to synthesize urchin-like NiS [11,12]. NiS hollow nanospheres were synthesized via γ-irradiation [13]. A sonochemical method [14] and a microemulsion system [15] produced NiS nanoparticles. Ghezelbash and Korgel [12] synthesized the $Ni_3S_4$ nanocrystal by the thermal decomposition of $NiCl_2$ and elemental sulfur in oleylamine. The same group reported the solventless thermolysis of a nickel alkylthiolate molecular precursor, producing nanorods and triangular nanoprisms of NiS [16]. Thermal decomposition of single-source precursors such as alkyl xanthates [17] and their pyridine adducts [18], mercaptobenzothiazole [19], (tetramethylethylenediamine)Ni($SCOC_6H_5$) [20], 1,1,5,5-tetra-iso-propyl-2-thiobiuret [21] and polysulfide [Ni(*N*-methylimidazole)$_6$]$S_8$ [22] in a hot coordinating solvent formed a mixture of rods and spheres of NiS, ellipsoidal NiS nanoparticles, alpha or beta NiS nanocrystals, and $NiS_2$ or $Ni_{1-x}S$ nanocrystals, respectively. Additionally, template-promoted growth was reported for NiS nanoparticles by Morris and co-workers [23] where NiS nanoparticles were grown on anodic alumina templates by decomposing nickel xanthate complex in supercritical $CO_2$ at 450 °C. Also, hollow spheres of NiS were synthesized using silica nanospheres as templates [24]. Another method deploying $Na_2SO_4$ or $Na_2S$ was used to sulfurize $Ni(OH)_2$ in a Teflon-lined autoclave at 180 °C for the synthesis of NiS hollow spheres [25]. A thermal decomposition method for different stoichiometries of nickel sulfide nanostructures was also reported by Tatsumisago and co-workers [26].

Recently, multimetallic assemblies have been prepared using a piperazine-based dithiocarbamate building block and Ni(dppe)$Cl_2$ by Wilton-Ely and co-workers [27]. These system have been utilized for the functionalization of gold nanoparticles [28]. However,

* Corresponding author. Tel.: +91 (0) 9451891030.
*E-mail addresses:* abhinavmarshal@gmail.com, kumar_abhinav@lkouniv.ac.in (A. Kumar).

http://dx.doi.org/10.1016/j.ica.2014.02.038
0020-1693/

to the best of our knowledge and findings, $[Ni(dppe)dtc]^+X^-$ species have never been explored as possible single-source precursor for the nickel sulfides.

With these viewpoints and in the quest for new precursors for the nickel sulfides having different morphologies herein we wish to report the synthesis, characterization and thermal decomposition products of the heteroleptic complex cation $[Ni\{S_2CN(CH_2)_4CHOH\}(dppe)]^+$ with different counter anions viz. $PF_6^-$, $BPh_4^-$ and $BF_4^-$.

## 2. Experimental

### 2.1. Materials and physical measurements

All the synthetic manipulations were performed under ambient atmosphere. The solvents were dried and distilled before use by following standard procedures. $^1H$, $^{13}C$ and $^{31}P$ NMR spectra were recorded on JEOL AL300 FTNMR spectrophotometers. Chemical shifts were reported in parts per million using TMS as internal standard for $^1H$ and $^{13}C$ NMR and phosphoric acid for $^{31}P$ NMR. Elemental analysis was performed on Exeter analytical Inc. "Model CE-440 CHN analyser". The structural characterization of the nickel sulfide were done using X-ray diffraction (XRD) measurements using Bruker AXS D8 Discover X-ray diffractometer, with Ni-filtered Cu K$\alpha_1$ radiation ($\lambda$ = 1.5405 Å). Small quantities of the decomposed products were dispersed in ethanol by sonicating for about 3 min. 5 mL of the suspension was placed on copper grids using a microliter pipette for SEM measurements that was carried out using a Hitachi S-4800 scanning electron microscope. For UV–Vis and photoluminescence measurements the nickel sulfides were dispersed in ethanol by sonicating for about 3 min. The UV–Vis and photoluminescence spectra for the complex precursors in dichloromethane solution and the obtained nickel sulfides by thermal decomposition of precursors were obtained using Shimadzu UV–Vis–NIR spectrophotometer (Model UV-3600) and Shimadzu (RF-5301 PC) spectrophotometer, respectively. The precursor $[Ni(dppe)Cl_2]$ was prepared in accordance with the literature procedure [29].

### 2.2. Syntheses of $[Ni\{S_2CN(CH_2)_4CHOH\}(dppe)]^+X^-$ ($X^-$ = $PF_6$ (**1**), $BPh_4$ (**2**), $BF_4$ (**3**))

4-Hydroxypiperidine (0.102 g, 1.01 mmol) was dissolved in anhydrous THF (10 mL) and to it was added NaOH (0.040 g, 1.00 mmol) dissolved in water (0.5 mL). The mixture was stirred for 10 min and then $CS_2$ (0.091 g, 1.20 mmol) was added. The mixture was stirred for additional 30 min until the color of the solution became yellow. To the yellow-coloured dithiocarbamate solution was added $NH_4PF_6$ (0.326 g, 2.00 mmol)/$NaBPh_4$ (0.684 g, 2.00 mmol)/$NH_4BF_4$ (0.208 g, 1.98 mmol) dissolved in methanol (10 mL) with vigorous stirring. To the resulting mixture $Ni(dppe)Cl_2$ (0.528 g, 1.03 mmol) dissolved in dichloromethane (35 mL) was added dropwise and the solution was additionally stirred for another 1 h and then vacuum evaporated to dryness. The residual mass was dissolved in dichloromethane (5 mL) and filtered through Celite and petroleum ether (50 mL) was added to precipitate the orange yellow-coloured residue.

$[Ni\{S_2CN(CH_2)_4CHOH\}(dppe)]PF_6{\cdot}CH_2Cl_2$ (**1**) (0.639 g, yield 74%); m.p. 237 °C. $^1H$ NMR ($CDCl_3$, $\delta$): 7.56–7.26 (m, 20H, $C_6H_5$), 5.30 (s, 1H, –OH), 3.87 (s, 2H, $-CH_{ax}$), 3.68 (s, 2H, $-CH_{eq}$), 2.09 (br. s, 4H, $-CH_2-CH_2-$), 2.03 (s, 2H, $-CH_{ax}$) 1.87 (s, 2H, $-CH_{eq.}$), 1.73 (s, 1H, $-CH_{ax}$). $^{13}C$ NMR ($CDCl_3$, $\delta$): 199.8 ($-NCS_2$), 138.2, 132.4, 129.5 (P–$C_6H_5$), 64.8, 47.9, 33.8 (piperdine), 25.6 ($-CH_2-CH_2-$). $^{31}P$ NMR ($CDCl_3$, $\delta$): 62.06 (dppe), −142.77 ($PF_6^-$) $^1J$(PF) 708.71 Hz. $\nu_{max}$(KBr)/$cm^{-1}$ 3437 (–OH), 1435 (C=N), 1103 (C–S). *Anal.* Calc. for $C_{33}H_{37}Cl_2F_6NNiOP_3S_2$: C, 45.32; H, 4.31; N, 1.62; S, 7.42. Found: C, 45.92; H, 4.34; N, 1.69; S, 7.52%. $\Lambda_M$ 113 $cm^2$ S $mol^{-1}$ in $10^{-3}$ M dichloromethane solution.

$[Ni\{S_2CN(CH_2)_4CHOH\}(dppe)]^+BPh_4{\cdot}CH_2Cl_2$ (**2**) (0.840 g, yield 81%); m.p. 231 °C. $^1H$ NMR ($CDCl_3$, $\delta$): 7.76–7.16 (m, 40H, $C_6H_5$), 5.32 (s, 1H, –OH), 3.84 (s, 2H, $-CH_{ax}$), 3.65 (s, 2H, $-CH_{eq}$), 2.12 (br. s, 4H, $-CH_2-CH_2-$), 2.06 (s, 2H, $-CH_{ax}$) 1.92 (s, 2H, $-CH_{eq.}$), 1.79 (s, 1H, $-CH_{ax}$). $^{13}C$ NMR ($CDCl_3$, $\delta$): 199.5 ($-NCS_2$), 140.1, 138.2, 134.2, 132.4, 129.8, 129.5 ($C_6H_5$), 64.8, 47.9, 33.8 (piperdine), 25.6 ($-CH_2-CH_2-$). $^{31}P$ NMR ($CDCl_3$, $\delta$): 62.04 (dppe). $\nu_{max}$(KBr)/$cm^{-1}$ 3435 (–OH), 1435 (C=N), 1103 (C–S). *Anal.* Calc. for $C_{57}H_{57}BCl_2NNiOP_2S_2$: C, 65.92; H, 5.53; N, 1.35; S, 6.18. Found: C, 66.01; H, 5.58; N, 1.46; S, 6.48%. $\Lambda_M$ 110 $cm^2$ S $mol^{-1}$ in $10^{-3}$ M dichloromethane solution.

$[Ni\{S_2CN(CH_2)_4CHOH\}(dppe)]^+BF_4.CH_2Cl_2$ (**3**) (0.563 g, yield 70%); m.p. 241 °C. $^1H$ NMR ($CDCl_3$, $\delta$): 7.55–7.23 (m, 20H, $C_6H_5$), 5.28 (s, 1H, –OH), 3.84 (s, 2H, $-CH_{ax}$), 3.63 (s, 2H, $-CH_{eq}$), 2.02 (br. s, 4H, $-CH_2-CH_2-$), 1.99 (s, 2H, $-CH_{ax}$) 1.83 (s, 2H, $-CH_{eq.}$), 1.73 (s, 1H, $-CH_{ax}$). $^{13}C$ NMR ($CDCl_3$, $\delta$): 199.8 ($-NCS_2$), 138.2, 132.4, 129.5 (P–$C_6H_5$), 64.8, 47.9, 33.8 (piperdine), 25.6 ($-CH_2-CH_2-$). $^{31}P$ NMR ($CDCl_3$, $\delta$): 63.67. $\nu_{max}$(KBr)/$cm^{-1}$ 3403 (–OH), 1434 (C=N), 1081 (C–S). *Anal.* Calc. for $C_{33}H_{37}BCl_2F_4NNiOP_2S_2$: C, 49.17; H, 4.63; N, 1.74; S, 7.96. Found: C, 49.83; H, 4.68; N, 1.86; S, 8.10%. $\Lambda_M$ = 115 $cm^2$ S $mol^{-1}$ in $10^{-3}$ M dichloromethane solution.

### 2.3. Preparation of nickel sulfides

The decomposition of precursor complex salts **1**, **2** and **3** were performed at 500 °C for 5 h in argon gas atmosphere in tubular furnace (with heating rate of 10 °C $min^{-1}$). The obtained nickel sulfides were washed thrice with de-ionised water (15 mL) and air-dried.

### 2.4. X-ray crystallography

Intensity data for **2** was collected at 150(2) K on a Nonius Kappa CCD diffractometer system equipped with graphite monochromated Mo K$\alpha$ radiation $\lambda$ = 0.71073 Å. The final unit cell determination, scaling of the data, and corrections for Lorentz and polarization effects were performed with Denzo-SMN [30]. The structures were solved by direct methods (SIR97) [31] and refined by a full-matrix least-squares procedure based on $F^2$ [32]. All non-hydrogen atoms were refined anisotropically; hydrogen atoms were located at calculated positions and refined using a riding model with isotropic thermal parameters fixed at 1.2 times the $U_{eq}$ value of the appropriate carrier atom.

Crystal data: $C_{113}H_{110}B_2Cl_2N_2Ni_2O_2P_4S_4$, $M$ = 1990.09, triclinic, $P\bar{1}$, $a$ = 9.3157(3) Å, $b$ = 14.5509(5) Å, $c$ = 19.4084(7) Å, $\alpha$ = 101.346(2), $\beta$ = 90.936(2), $\gamma$ = 91.9370(10) $V$ = 2577.25(15) $Å^3$, $Z$ = 1, $D_{calc}$ = 1.282 mg $m^{-3}$, $F(000)$ = 1042, crystal size 0.30 × 0.10 × 0.05 mm, reflections collected 25741, independent reflections 9291 [$R$(int) = 0.0724], Final indices [$I > 2\sigma(I)$] $R_1$ = 0.0704 $wR_2$ = 0.1585, $R$ indices (all data) $R_1$ = 0.1014, $wR_2$ = 0.1739, Goodness-of-fit (GOF) on $F^2$ 1.099, Largest difference peak and hole 1.263 and −0.476 e $Å^{-3}$.

## 3. Results and discussion

### 3.1. Synthesis

All the three $[Ni\{S_2CN(CH_2)_4CHOH\}(dppe)]^+X^-$ ($X^-$ = $PF_6$ (**1**), $BPh_4$ (**2**), $BF_4$ (**3**)) compounds were obtained by addition of stoichiometric amounts of $Ni(dppe)Cl_2$, 4-piperidinoldithiocarbamate and the counter anions $PF_6^-$, $BPh_4^-$, $BF_4^-$ in THF, methanol and dichloromethane mixture (Scheme 1). All the three compounds

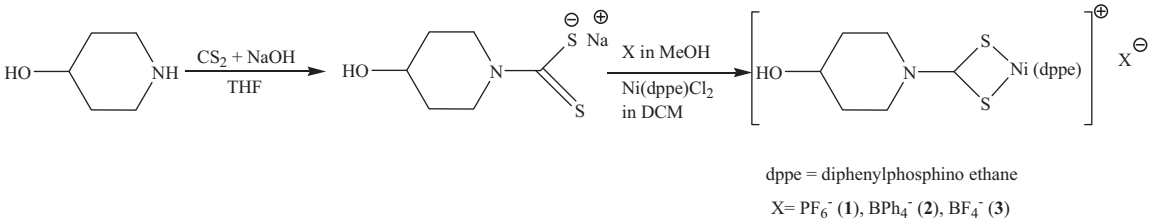


**Scheme 1.** Synthesis of the complexes.

were air-stable and soluble in halogenated solvents but insoluble in petroleum ether. Crystals of **2**, and **3** suitable for X-ray analysis were obtained by slow evaporation of dichloromethane–methanol mixture. For all the three complexes the observed $\Lambda_M$ lying in the range of $\Lambda_M$ 110–115 $cm^2\,S\,mol^{-1}$ in $10^{-3}$ M dichloromethane solution shows their 1:1 electrolytic behavior [33].

### 3.2. Spectroscopy

The purity and composition of the three complexes were checked by $^1H$ NMR spectroscopy. The presence of signals in the range $\delta$ 7.76–7.16 ppm indicates the presence of aromatic protons of the dppe for all the three compounds and $BPh_4^-$ anion in the case of **2**. Additionally, the other $^1H$ NMR signals corresponds to the piperdine moiety and ethyl fragment of dppe. In $^{13}C$ NMR the signal at $\sim\delta$ 199 ppm correspond to the $NCS_2$ function and the signals in the range of $\delta$ 140–130 ppm corresponds to the aromatic carbons of the dppe ligand for all the three systems and $BPh_4^-$ anion in the case of **2**. In $\{^1H\}^{31}P$ NMR spectra of the complexes the signal at $\sim\delta$ 62 ppm indicates that both phosphorus donors of the dppe ligands are magnetically equivalent. Additionally, in the case of **1**, the septet centered at $\delta$ −142.77 ($PF_6^-$) $^1J(PF)$ 708.71 Hz corresponds to the phosphorus centre of the $PF_6^-$.

The IR spectra of all the complexes show a distinct vibrational band around ~1100 $cm^{-1}$ which is associated with the symmetric bidentate $\nu(CS_2)$ vibration of the dithiocarbamate ligand. The band near 1435 $cm^{-1}$ for all the complexes is characteristic of the thioureide vibration and is associated with the $\nu$(C–N) which is appreciably higher than the free ligand and thereby indicates significant increase in the partial double bond character of C–N bond. Additionally, the band at ~3435 $cm^{-1}$ is indicative of the free –OH function in the piperidinol moiety.

The electronic spectra for all of the three compounds were recorded in dichloromethane (Fig. 1). In all the three cases the bands observed below 230–400 nm are mainly the ligand centered and $\pi\rightarrow\pi^*$ and intraligand charge transfer transition [34,35]. The very weak broad absorptions at 400 nm is assignable to L→M, ligand-to-metal charge transfer (LMCT) transitions consistent with square planar geometry about the metal center [36]. When excited at 300 nm all the three compounds display broad emissions at ~450 nm which arises from intraligand charge transfer [34].

### 3.3. Molecular structure description

The molecular structure of complex **2** with atomic numbering scheme is shown in Fig. 2. The complex **2** crystallizes in triclinic system with $P\bar{1}$ space group. The $[Ni\{S_2CN(CH_2)_4CHOH)\}(dppe)]$ core is cationic and a $B(C_6H_5)_4^-$ anion is also present in the system for neutrality. Additionally dichloromethane solvent undergoes co-crystallization within the unit cell. There is half a $CH_2Cl_2$ per molecular unit (though the microanalysis fits better for a whole solvent which suggests variable amounts). The immediate distorted square planar geometry around the Ni(II) center is defined by two sulfur atoms S(1), S(2) of the dithiocarbamate ligand and P(1) and P(2) of the dppe. The Ni–S and Ni–P bond distances lie in the range of 2.2021(13)–2.2162(13) and 2.1617(13)–2.1706(13) Å, respectively which indicates almost symmetrical bidentate behavior of both dithiocarbamate and dppe ligands. Within the dithiocarbamate function, $C–N_{dtc}$ bond length of 1.314(6) Å indicates a substantial delocalization of the π-electron density in these bonds [37]. The S(1)–Ni–S(2) bite angle of 79.72(5)° in the four membered chelate ring shows small distortion from the square planar geometry. The bite angle P(1)–Ni–P(2) for five membered ring is 86.74(5)° and offers significantly lower distortion for the square planar geometry because of the relatively greater flexibility. The dihedral angle between the planes formed by the four- and five-membered chelate ring is 10.10°.

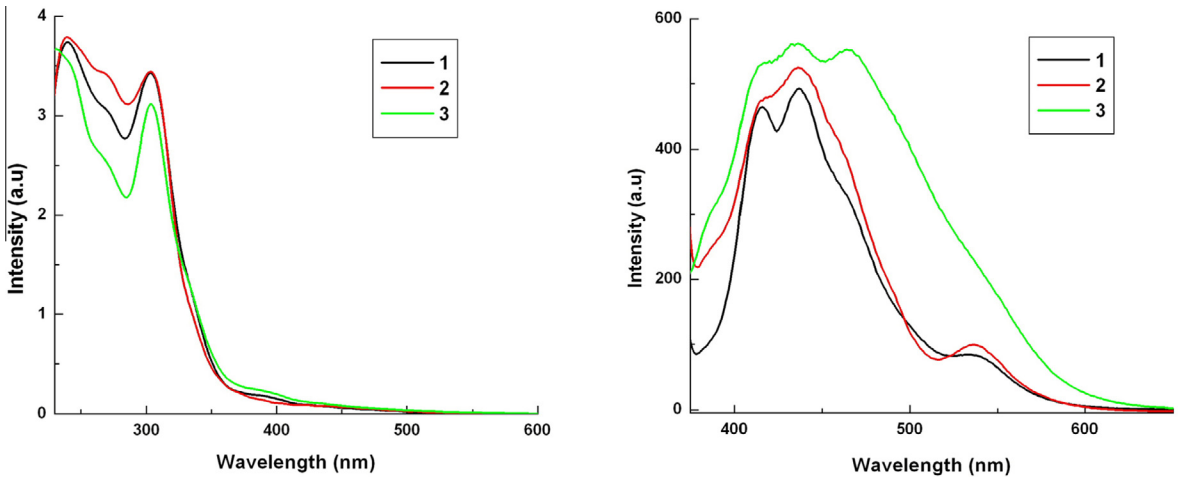


**Fig. 1.** Electronic absorption (left) and photoluminescence (right) spectra of the complexes in $10^{-3}$ M dichloromethane solution.

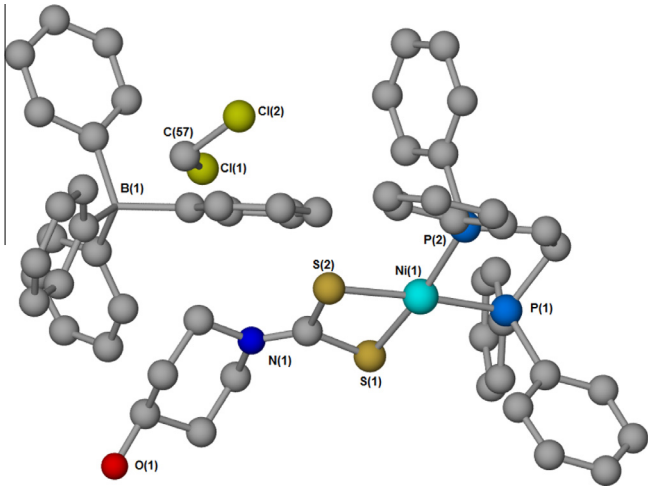


**Fig. 2.** Perspective view of molecular structure of **2**. Hydrogen atoms have been omitted for clarity.

**Table 1**
Selected bond lengths and bond angles for complex **2**.

| Bond lengths (Å) | | Bond angles (°) | |
|---|---|---|---|
| Ni(1)–S(1) | 2.2021(13) | S(1)–Ni(1)–S(2) | 79.72(5) |
| Ni(1)–S(2) | 2.2162(13) | P(1)–Ni(1)–P(2) | 86.74(5) |
| Ni(1)–P(1) | 2.1617(13) | S(1)–C(1)–S(2) | 110.2(3) |
| Ni(1)–P(2) | 2.1706(13) | | |
| N–C(1) | 1.314(6) | | |
| C(1)–S(1) | 1.720(5) | | |
| C(1)–S(2) | 1.732(5) | | |
| C(7)–P(1) | 1.836(5) | | |
| C(8)–P(2) | 1.823(5) | | |

The six-membered piperidine ring adopts the chair conformation. Selected metrical parameters for **1** are presented in Table 1.

### 3.4. TGA–DTA

Thermal decomposition of the complexes **1**–**3** was performed under nitrogen atmosphere (Fig. 2). The TGA profile in all the three cases displays two-step decomposition. The first weight loss occurs around 100 °C which corresponds to the loss of solvents present within the crystal lattice. The second weight loss starts at around 300 °C and leads to the formation of Ni–S phases around 400 °C; two components to this stage can be discerned, most clearly in traces for **2** and **3** where inflections in the TGA can be seen at *ca.* 350 °C. The residue% from the TGA plots for complex **1**–**3** were found to be *ca.* 15.7%, 13.5% and 11.2%, respectively. The calculated residual mass corresponding to the formation of $NiS_2$ at the end of decomposition in case of complex **1** was found to be 14.2% which is in good agreement with observed value of 15.7%. The small difference in the observed and calculated values may be because of the formation of an impurity phase as suggested by X-ray diffraction studies (*vide infra*). In the case of **2**, calculated residues for NiS and $NiS_2$ are 9.7% and 11.7%, respectively. Both the calculated values are lower than the observed value of 13.5%. The probable reason may be the presence of an amorphous impurity. Also for **2**, the initial weight loss corresponding to the solvent loss suggests that more than one solvent might be present as it does not display a single clear step. For **3**, the observed residual weight in TGA is 11.2%. The calculated residual weights corresponding to residues of $NiS_2$ and NiS were found to be 14.2% and 10.5%, respectively. Although the residual% is more close to NiS, the X-ray diffraction pattern shows that $NiS_2$ is formed at the end of decomposition. This may suggest that precursor **3** has some volatility, possibly arising from the presence of the fluorinated anion (Fig. 3).

### 3.5. PXRD and SEM

The powder X-ray diffraction patterns of the nickel sulfides obtained by decomposing precursors **1**–**3** at 500 °C are presented in Fig. 4. All the samples could be indexed to Ni–S phases. The powder X-ray diffraction patterns of **1** and **3** matched with triclinic $NiS_2$ (JCPDS 73-0574) and cubic $NiS_2$ (JCPDS 80-0375), respectively. The refined lattice parameters for **1** and **3** were found to be $a = 3.594(4)$; $b = 5.623(8)$; $c = 16.61(2)$ Å and $a = b = c = 5.6748(4)$ Å, respectively. Sample **2** could be indexed to hexagonal NiS (JCPDS 77-1624) phase with refined lattice parameters; $a = b = 3.3778(9)$; $c = 5.262(4)$ Å. The Le Bail refinement [38] was done using FULLPROF programme [39,40]. The impurity phases were also found in all the three samples but least in the sample **2**. Since in all the three cases, Ni–S phases were formed, therefore, it can be concluded that the present method is suitable for the synthesis of nickel sulfides from a single source precursor.

SEM micrographs for the decomposed products obtained from **1** to **3** indicate the formation of agglomerated sheets in the case of **1**, rods in **2** and aggregated globules in **3** (Fig. 5).

### 3.6. UV–Vis absorption and photoluminescence

The UV–Vis absorption spectra for the three nickel sulfides samples **1**–**3** are presented in Fig. 6. All the three sulfides display strong absorption in the UV region around 200 nm and a weak absorption peak around 300 nm. The sample **3** exhibited an absorption tail in the visible region with weak absorptions around 400, 550 and 700 nm. The corresponding photoluminescence spectra are also shown in Fig. 6. On excitation at 274 nm, emission around 360 nm was observed for the **1** with an additional shoulder emission around 340 nm. Sample **2** showed emission around 435 nm with a shoulder

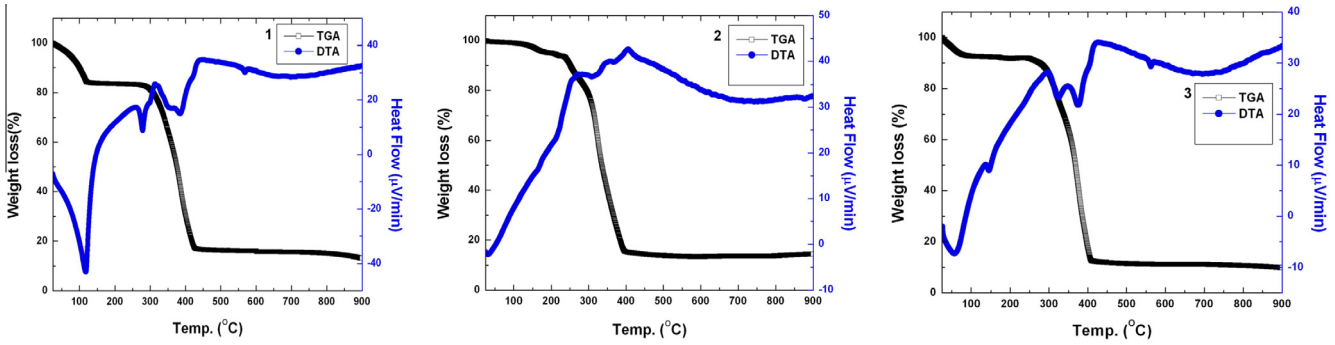


**Fig. 3.** TGA–DTA curves for the complexes **1**–**3**.

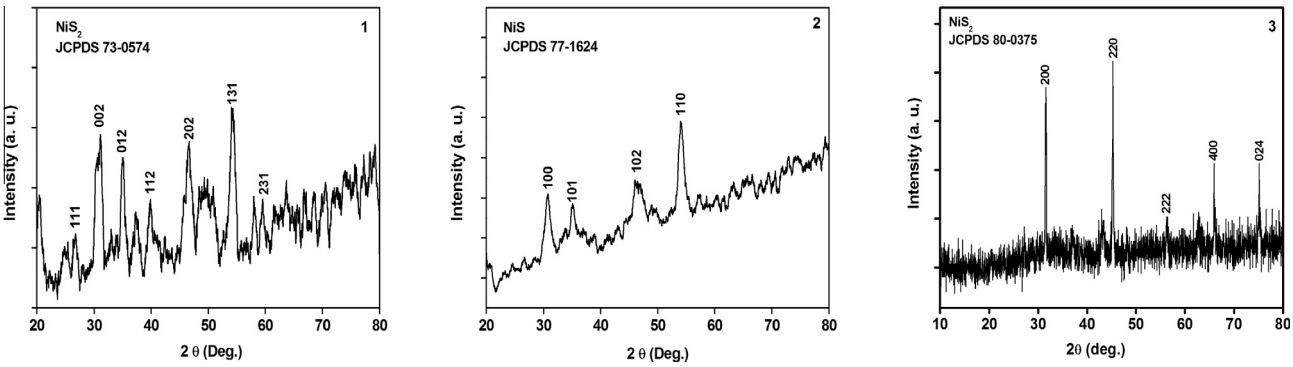


**Fig. 4.** Powder X-ray diffractograms of the nickel sulfides obtained by the decomposition of the precursors at 500 °C for 6 h.

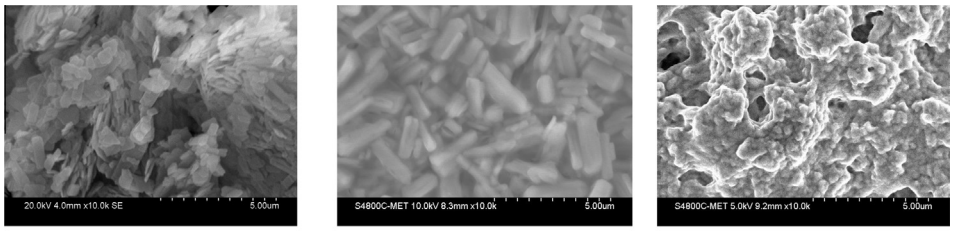


**Fig. 5.** SEM micrographs for the obtained nickel sulfides obtained from the precursors **1**–**3**.

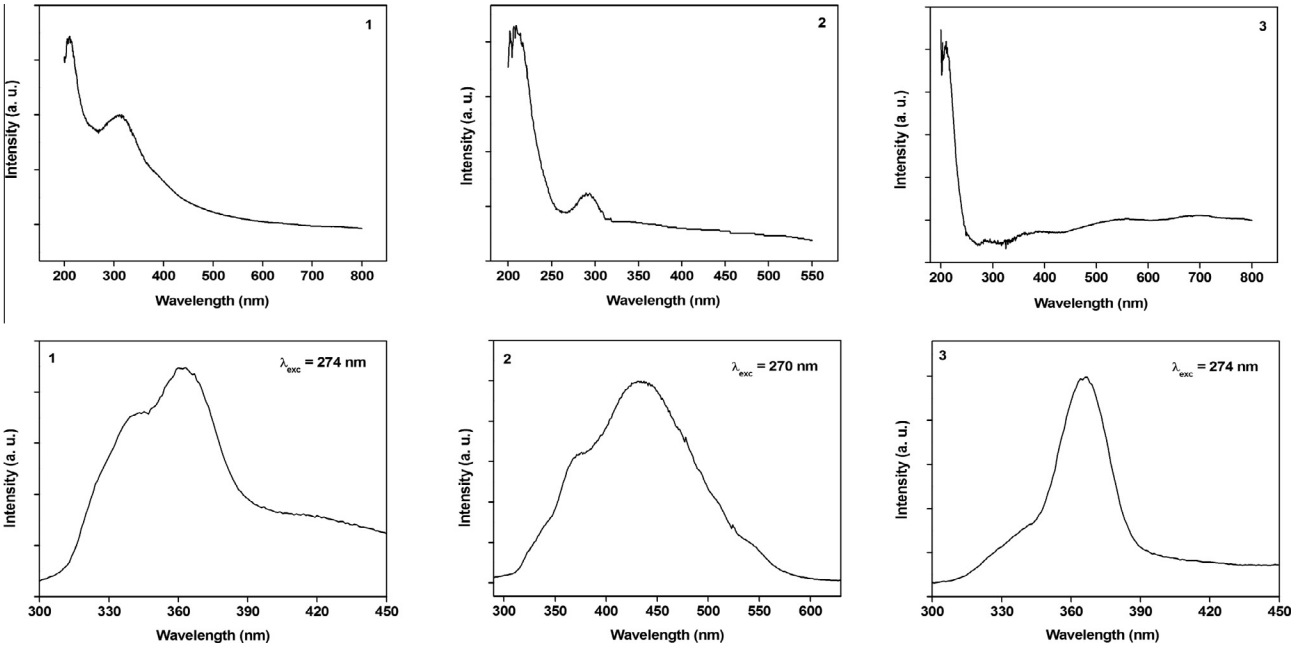


**Fig. 6.** UV–Vis (above) and photoluminescence (below) spectra of the nickel sulfides obtained from the precursors **1**–**3**.

at 372 nm, when excited at 270 nm. The broad emission peaks in **1** (340 and 360 nm) and **2** (372 and 435 nm) may be due to electronic transitions caused by defects in the interfacial region, [41,42] whereas for the sample **3**, emission around 370 nm was recorded for excitation wavelength, 274 nm.

## 4. Conclusions

From the aforementioned investigations it can be concluded that the $[Ni\{S_2CN(CH_2)_4CHOH\}(dppe)]^+X^-$ is a potential candidate as a single-source precursor for the nickel sulfides. Additionally in these types of ionic complex systems one can alter the nature and bulkiness of the counter-anion which assist in the growth of different phases of nickel sulfides with different morphologies.

## Acknowledgements

AK and RC are thankful to the Department of Science and Technology, New Delhi for financial support in the form of Project no. SB/FT/CS-018/2012 and IFA12-CH-34, respectively.

## Appendix A. Supplementary material

CCDC 970436 contains the supplementary crystallographic data for this paper. These data can be obtained free of charge from The Cambridge Crystallographic Data Centre via www.ccdc.cam.ac.uk/data_request/cif. Supplementary data associated with this article can be found, in the online version, at http://dx.doi.org/10.1016/j.ica.2014.02.038.

## References

[1] G. Andersen, P. Kofstad, Oxid. Met. 43 (1995) 173.
[2] R.D. Tilley, D.A. Jefferson, J. Phys. Chem. B 106 (2002) 10895.
[3] A. Manthiram, Y.U. Jeong, J. Solid State Chem. 147 (1999) 679.
[4] H.T. Zhang, G. Wu, X.H. Chen, Mater. Lett. 59 (2005) 3728.
[5] K. Anuar, Z. Zainal, N. Saravanan, S. Nor, Hamizi, J. Indian Chem. Soc. 82 (2005) 526.
[6] H. Vandenborre, P. Vermeiren, R. Leysen, Electrochim. Acta 29 (1984) 297.
[7] J.Z. Wang, S.L. Chou, S.Y. Chew, J.Z. Sun, M. Forsyth, D.R. MacFarlane, H.K. Liu, Solid State Ionics 179 (2008) 2379.
[8] G. Kishan, L. Coulier, V.H.J. de Beer, J.A.R. van Veen, J.W. Niemantsverdriet, J. Catal. 196 (2000) 180.
[9] W.M. Kriven, J. Am. Ceram. Soc. 71 (1988) 1021.
[10] C. Wadia, A.P. Alivisatos, D.M. Kammen, Environ. Sci. Technol. 43 (2009) 2072.
[11] W. Zhang, L. Xu, K. Tang, F. Li, Y. Qian, Eur. J. Inorg. Chem. 4 (2005) 653.
[12] A. Ghezelbash, B.A. Korgel, Langmuir 21 (2005) 9451.
[13] Y. Hu, J. Chen, W. Chen, X. Lin, X. Li, Adv. Mater. 15 (2003) 726.
[14] H. Wang, J.R. Zhang, X.N. Zhao, S. Xu, J.J. Zhu, Mater. Lett. 55 (2002) 253.
[15] P.S. Khiew, N.M. Huang, S. Radiman, Md. S. Ahmad, Mater. Lett. 58 (2004) 762.
[16] A. Ghezelbash, M.B. Sigman, B.A. Korgel, Nano Lett. 4 (2004) 537.
[17] N. Pradhan, B. Katz, S. Efrima, J. Phys. Chem. B 107 (2003) 13843.
[18] N. Alam, M.S. Hill, G. Kociok-Kohn, M. Zeller, M. Mazar, K.C. Molloy, Chem. Mater. 20 (2008) 6157.
[19] B. Geng, X. Liu, J. Ma, Q. Du, Mater. Sci. Eng., B 145 (2007) 17.
[20] L. Tian, L.Y. Yep, T.T. Ong, J. Yi, J. Ding, J.J. Vittal, Cryst. Growth Des. 9 (2009) 352.
[21] A.L. Abdelhady, M.A. Malik, P. O'Brien, F. Tuna, J. Phys. Chem. C 116 (2012) 2253.
[22] J.H.L. Beal, P.G. Etchegoin, R.D. Tilley, J. Phys. Chem. C 114 (2010) 3817.
[23] L. Barry, J.D. Holmes, D.J. Otway, M.P. Copley, O. Kazakova, M.A. Morris, J. Phys.: Condens. Matter 22 (2010) 76001.
[24] T. Zhu, Z. Wang, S. Ding, J.S. Chen, X.W. Lou, RSC Adv. 1 (2011) 397.
[25] Y. Wang, Q. Zhu, L. Tao, X. Su, J. Mater. Chem. 21 (2011) 9248.
[26] K. Aso, H. Kitaura, A. Hayashi, T. Tatsumisago, J. Mater. Chem. 21 (2011) 2987.
[27] J.D.E.T. Wilton-Ely, D. Solanki, E.R. Knight, K.B. Holt, A.L. Thompson, G. Hogarth, Inorg. Chem. 47 (2008) 9642.
[28] E.R. Knight, E.R. Leung, Y.H. Lin, A.R. Cowley, D.J. Watkin, A.L. Thompson, G. Hogarth, J.D.E.T. Wilton-Ely, Dalton Trans. (2009) 3688.
[29] R. Busby, M.B. Hursthouse, P.S. Jarrett, C.W. Lehmann, K.M.A. Malik, C. Phillips, J. Chem. Soc., Dalton Trans. (1993) 3767.
[30] Z. Otwinowski, W. Minor, in: C.W. Carter Jr., R.M. Sweet (Eds.), Methods in Enzymology, vol. 276, Academic, San Diego, 1997, p. 307.
[31] A. Altomare, M.C. Burla, M. Camalli, G.L. Cascarano, C. Giacovazzo, A. Guagliardi, A.G.G. Moliterni, G. Polidori, R. Spagna, J. Appl. Crystallogr. 32 (1999) 115.
[32] G.M. Sheldrick, Acta Crystallogr., Sect. A 64 (2008) 112.
[33] W.J. Geary, Coord. Chem. Rev. 7 (1971) 81.
[34] S.P. Kaiwar, A. Vodacek, N.V. Blough, R.S. Pilato, J. Am. Chem. Soc. 119 (1997) 3311.
[35] E.G. Bakalbassis, G.A. Katsoulos, C.A. Tsipis, Inorg. Chem. 26 (1987) 3151.
[36] R.S. Amim, M.R.L. Oliveira, G.J. Perpetuo, J. Janczak, L.D.L. Miranda, M.M.M. Rubinger, Polyhedron 27 (2008) 1891.
[37] K.A. Wheeler, B. Harrington, M. Zapp, E. Casey, Cryst. Eng. Commun. 5 (2003) 337.
[38] A. Le Bail, H. Duroy, J.L. Fourquet, Mater. Res. Bull. 23 (1988) 447.
[39] J. Rodriguez-Carvajal, FULLPROF: A Program for Rietveld Refinement and Pattern-matching Analysis, Abstracts of Satellite Meeting on Powder Diffraction, Congr. Int. Union of Crystallography, Toulouse, France, 1990, p. 127.
[40] J. Rodriguez-Carvajal, Physica B 192 (1993) 55.
[41] H. Li, L. Chai, X. Wang, X. Wu, G. Xi, Y. Liu, Y.T. Qian, Cryst. Growth Des. 7 (2007) 1918.
[42] M. Salavati-Niasari, M. Bazarganipour, F. Davar, J. Alloys Compd. 489 (2010) 530.